

# Electric field measurements in noctilucent clouds

Robert H. Holzworth

Earth and Space Sciences, University of Washington, Seattle, Washington, USA

Richard A. Goldberg

Laboratory for Extraterrestrial Physics, NASA Goddard Space Flight Center, Greenbelt, Maryland, USA

Received 18 December 2003; revised 11 May 2004; accepted 1 June 2004; published 18 August 2004.

[1] Two rockets were flown through noctilucent clouds (NLC) during the Distribution and Role of Particles in the Polar Summer Mesosphere using Coordinated Rocket, Radar, and Lidar Techniques (DROPPS) rocket experiment from Andøya Rocket Range, Norway, in July 1999. Each rocket was equipped with three-axis, double-double, high-impedance Langmuir probes (12 probes each flight) and produced unprecedented resolution of the electric potential distribution around the rockets in and near both a weak NLC (DROPPS1) and a very strong NLC (DROPPS2). Detailed analysis of the vehicle interaction during the weak NLC encounter, in which no large geophysical electric fields were detected [Holzworth *et al.*, 2001], provided a basis for understanding the strong NLC encounter by DROPPS2, where geophysical electric fields reached  $3 \text{ V m}^{-1}$ . The electric field orientation is shown to be vertically downward. In the case of the strong NLC encounter a layer of excess positive charge at the top of the layer reached a density of  $2 \text{ pC m}^{-3}$ , deduced from the sharp field gradient. The total integrated potential drop through the NLC was 2 kV.

**INDEX TERMS:** 2411 Ionosphere: Electric fields (2712); 2427 Ionosphere: Ionosphere/atmosphere interactions (0335); 3304 Meteorology and Atmospheric Dynamics: Atmospheric electricity;

**KEYWORDS:** noctilucent cloud, electric field

**Citation:** Holzworth, R. H., and R. A. Goldberg (2004), Electric field measurements in noctilucent clouds, *J. Geophys. Res.*, **109**, D16203, doi:10.1029/2003JD004468.

## 1. Introduction

[2] The role of electrodynamic phenomena in the development and persistence of both noctilucent clouds (NLCs) and polar mesospheric summer echoes (PMSEs) has become a widely debated subject (compare Cho and Kelley [1993], Zadorozhny *et al.* [1993], and Cho and Röttger [1997] and the recent series of papers by Holzworth *et al.* [2001], Pfaff *et al.* [2001], Croskey *et al.* [2001], and Mitchell *et al.* [2001]). Although extensive phenomenology (occurrence frequency or spatial extent) is known, the source mechanisms for these phenomena, and their relationship to the well-established presence of charged aerosols, are just becoming better understood [cf. Rapp *et al.*, 2003; Rapp and Lübken, 2003]. However, the importance of large-scale electric fields to these phenomena remains an outstanding topic and is the subject of this paper.

[3] During the Distribution and Role of Particles in the Polar Summer Mesosphere using Coordinated Rocket, Radar, and Lidar Techniques (DROPPS) experiment [cf. Goldberg *et al.*, 2001], rocket-borne measurements have been made to study the electric field structure of both NLC and PMSE. Holzworth *et al.* [2001] provide a detailed analysis of the first DROPPS rocket flight through a strong PMSE with a very weak NLC. They concluded that there

were no large geophysical electric fields observed during passage through the PMSE and through the weak NLC regions. Furthermore, with the use of a dozen independent, high-impedance Langmuir probes a detailed diagnosis was made of how the probes were perturbed by the charged wake of the rocket. Holzworth *et al.* [2001] showed that electric fields, determined with probes that were not in the wake, were uniformly small during the passage (less than a few tens of millivolts per meter) while also clearly identifying the perturbing influence of the charged wake of the rocket on the aft probes. Such a positively charged wake effect would be expected in the PMSE or NLC regions when the negative charge was mostly carried on aerosols (in the electron byteouts) so that the positive ions had the largest mobility of any charge carriers and filled the hole drilled in the mesosphere by the rocket faster than any other available charge carriers.

[4] In this paper we concentrate on the second DROPPS flight, in which a strong NLC was traversed, but no PMSE was detected. The DROPPS2 rocket, a Black Brant V launched 0328 UT on 14 July 1999 from Andøya Rocket Range, Norway, was extremely well instrumented to study electric and magnetic fields as well as charged particles (electrons, ions, and charged aerosols). These instruments have been described elsewhere [Goldberg *et al.*, 2001; Holzworth *et al.*, 2001; Pfaff *et al.*, 2001] and were identical for both DROPPS flights. As discussed by those authors, the first DROPPS flight was launched into an extremely

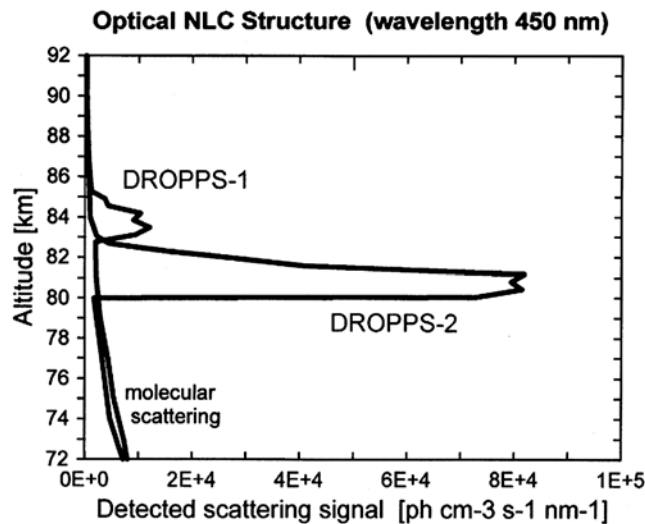


**Figure 1.** Volume scattering ratios during Distribution and Role of Particles in the Polar Summer Mesosphere using Coordinated Rocket, Radar, and Lidar Techniques (DROPPS)1 and DROPPS2 flights as determined from an analysis of the optical scattering as seen by the 450 nm photometer (arbitrary units, linear scale) [from *Gumbel, 2001*].

strong PMSE event with no ground-based evidence for an NLC. The flight instruments did record the passage of a weak NLC during the DROPPS1 flight, located within the lower portion of the PMSE region. In stark contrast to the conditions during the first flight, *Goldberg et al.* [2001] provided data showing that at the time of the DROPPS2 flight, there was no evidence of any PMSE. At the same time the Arctic Lidar Observatory for Middle Atmosphere Research (ALOMAR) Rayleigh, Mie, and Raman scattering (RMR) lidar recorded one of the stronger NLC events of the summer, which was confirmed by the DROPPS2 photometer [Gumbel, 2001]. Figure 1 presents a comparison of the volume scattering found during the two rocket flights [from *Gumbel, 2001*]. In Figure 1 the scattering of sunlight by the NLC is used to determine the relative NLC intensity with an altitude resolution of  $\sim 0.3$  km. The other geophysical difference noted during the two flights was that during DROPPS1, there was a small geomagnetic substorm under way, while during DROPPS2 the Andøya magnetometer was flat, indicating no auroral activity at the time of the second flight.

[5] Here we present electric field probe data for the second DROPPS flight in which we will demonstrate that unlike the first flight, DROPPS2 data give strong evidence for large geophysical electric fields in the NLC. Using upleg data, we will show that all our electric field sensors were operating properly and will demonstrate that the forward, outer probes exhibit no evidence of entering the charged wake, unlike the aft probes, which were saturated during much of the encounter. We conclude that the electric field reached  $3 \text{ V m}^{-1}$  vertically downward inside the NLC. We will use downleg data to directly confirm the upleg conclusion. From the gradient of the electric field we also conclude that there was a layer of excess positive charge at the top of

the NLC, with net charge density  $\rho = 2 \text{ pC m}^{-3}$  in a narrow layer just 10 m thick.

## 2. Instrumentation and Data

[6] The main subject of this paper concerns the electric field instrument, which included 12 boom-mounted, spherical, high-impedance Langmuir probes arranged in a “double-double” configuration, with two pairs of forward 3 m tip-to-tip axes and a single pair of aft booms (also giving maximum separation of 3 m tip-to-tip). Each boom had a probe at the end and a second probe 0.6 m inboard from the boom tip. Our analysis here will report probe voltage differences from a variety of probes, which are schematically shown in Figure 2. Our telemetry data includes both individual probe voltages relative to the rocket as well as differential voltages between various pairs of probes. The vehicle was oriented on the upleg with an attitude control system so that the rocket axis was parallel to the velocity vector as the rocket encountered the NLC layer; this was an angle of  $\sim 54^\circ$  elevation (above the horizontal). It was spinning at 2.2 Hz during the upleg NLC encounter and spun down to 1.2 Hz on the downleg.

[7] For the experimentalist, perhaps the best way to look at the evidence for geophysical electric fields is to look at probe voltage differences between the forward, outer pairs of probes  $V_{2-1}$  and  $V_{3-4}$  (for the voltage differences  $V_2 - V_1$  and  $V_3 - V_4$ , respectively). These probes are out in front of the rocket in the RAM direction and well out of the rocket wake (see *Gumbel* [2001] for an analysis of the supersonic wake around sounding rockets in the mesosphere). Figure 3

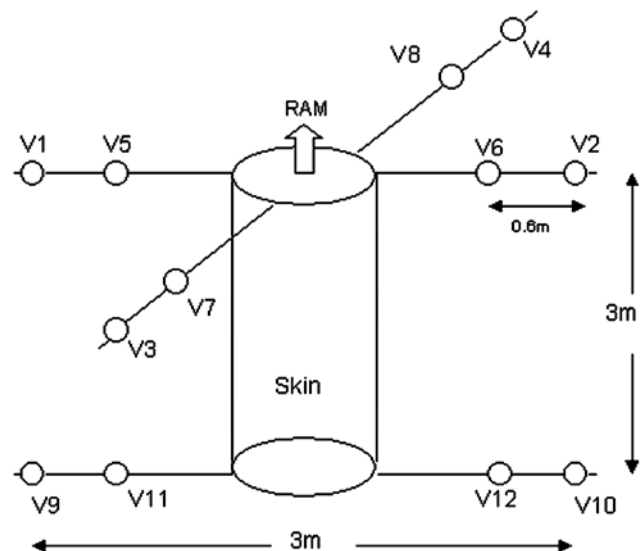


**Figure 2.** DROPPS electric Langmuir probe orientation and layout. Twelve independent probes were flown, eight on the forward end looking directly into the RAM direction and having an outermost separation of 3.0 m tip-to-tip. The inner probes on each boom are located 0.6 m inboard from the center of the outermost probes.  $V_{2-1}$  and  $V_{3-4}$  represent the primary measurements for geophysical fields and result from taking the difference between the voltage of probe 1 ( $V_2$  or  $V_3$ ) and subtracting that of probe 2 ( $V_1$  or  $V_4$ ), then providing some gain before transmitting the data to ground.

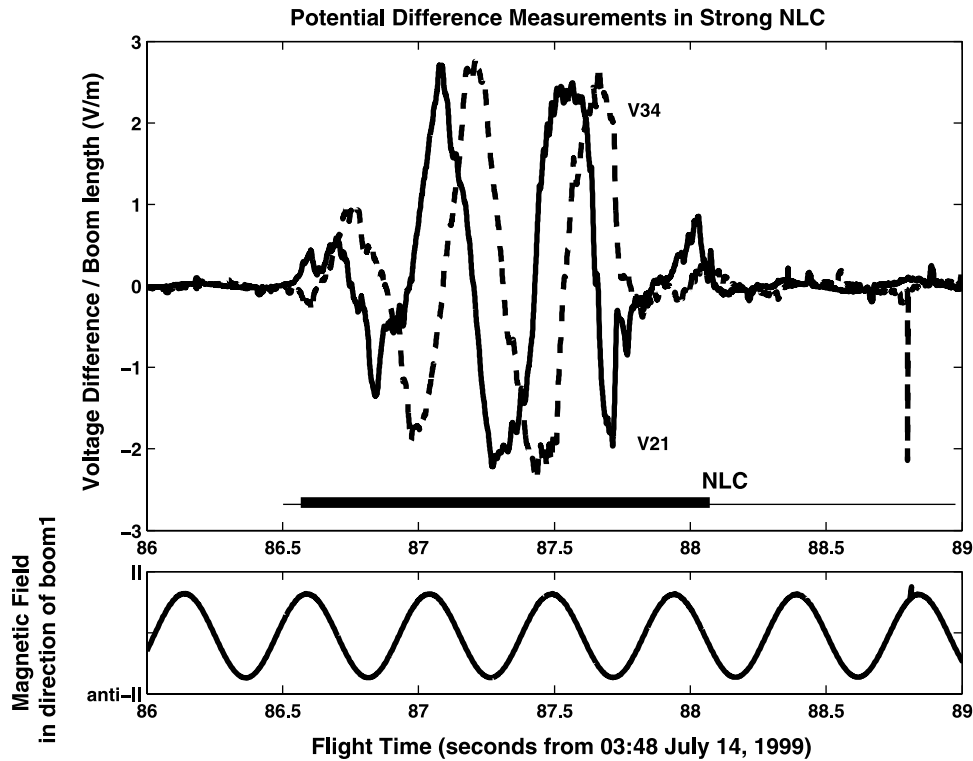


**Figure 3.** Three seconds of potential difference measurements from the forward probe pairs  $V_{2-1}$  and  $V_{3-4}$  during the DROPPS2 encounter with a strong noctilucent cloud (NLC). The lower trace is a signal proportional to the magnetic field in the direction of boom 1. The  $V_{2-1}$  and  $V_{3-4}$  traces show the expected  $90^\circ$  phase shift as these orthogonal boom axes rotate through the large DC field within the NLC.

provides these data, including one axis of the fluxgate magnetometer data which is proportional to the magnetic field in the direction of boom 1 (refer to Figure 2). Figure 3 (top) includes the potential difference measured between probes 2 and 1 ( $V_{2-1}$ ) and between probes 3 and 4 ( $V_{3-4}$ ). We have indicated the times of the enhanced volume scattering (from Figure 1); the thin line indicates weak scattering, which trails off more slowly above the main NLC.

[8] In Figure 3 we see that the voltage differences, in the rotating frame, appear as sine wave oscillations at the rocket spin period ( $\sim 0.45$  s). The two independent measurements  $V_{2-1}$  and  $V_{3-4}$  have the  $90^\circ$  phase relationship expected in a steady field with orthogonal axes. In the rocket frame the magnitude of the voltage difference grows slowly as the rocket enters the lower boundary of the NLC, taking a full spin to achieve maximum levels of  $\sim 8$  V peak-to-peak (or a field of  $> 2.5$  V m $^{-1}$ ). This peak magnitude is maintained for more than a full spin until the field cuts off abruptly (at 87.75 s) as the rocket passes the upper boundary of the NLC. Note that the peaks in the magnetic field along boom 1 (Figure 3 (bottom)) come shortly before the peaks seen in  $V_{2-1}$ . When this magnetic component peaks, it means that boom 1 is pointing as close to the magnetic field as possible in the spin plane. The magnetic field inclination is  $77^\circ$  below the horizontal, so this means the electric field is oriented nearly vertically downward. The same conclusion can be reached when examining  $V_{3-4}$ , which is a completely independent measurement. Therefore the electric field, as determined from the outer probes in the forward boom

plane, indicates that we passed through a downward vertical geophysical electric field of  $\sim 2\text{--}3$  V m $^{-1}$ .

[9] Another way to view these data is shown in Figure 4, in which the same data as in Figure 3 are used to determine the instantaneous electric field vector in the spin plane and are presented in a nonrotating, geographic reference frame. Clearly, the field is in the downward vertical direction as projected onto the spin plane. Each data point in Figure 4 is the tip of an electric field vector from the origin (0,0). When despinning these data for this plot, we used all the data, including nonfield perturbations such as caused by the Sun pulses when a probe is briefly shadowed by the rocket. Therefore some of the scatter in the horizontal direction may be caused by artifacts of the measurement. The main point of Figure 4 is that the electric field is vertically downward to at least  $\pm 20^\circ$ .

[10] Since there has been so much controversy over the existence, or not, of large mesospheric electric fields [Hale *et al.*, 1981; Maynard *et al.*, 1981; Zadorozhny *et al.*, 1993; Kelley *et al.*, 1983], it is important to provide further evidence that our interpretation of the probe data is correct. We will show that (1) the probes were both clearly working properly below and above the NLC layer, that (2) electric fields determined by shorter boom lengths (between probe pairs 1-5, 2-6, 3-7, and 4-8 (see Figure 2)) give the same electric field magnitude and orientation, and that (3) the downleg data are completely consistent with the upleg data, even though the rocket orientation was changed substantially for the downleg.

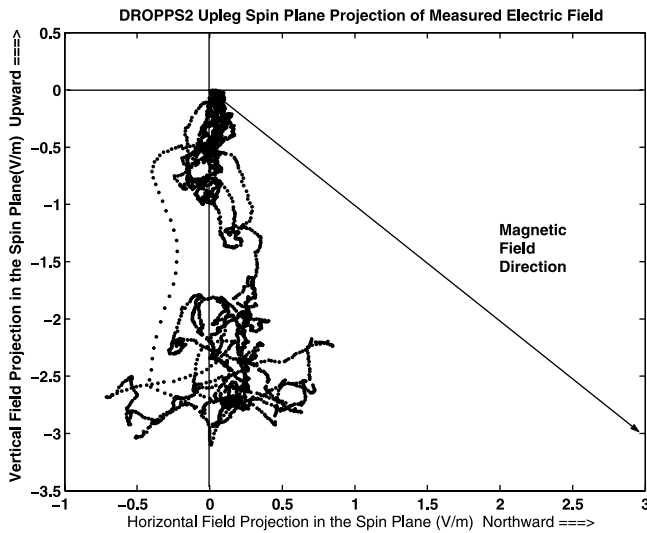


**Figure 4.** The same data as in Figure 3 presented in a geographic (despun) geometry with the horizontal axis pointing north (magnetic and geographic north is the same to within  $2^\circ$ ). The vertical axis gives the vertical direction. Each data point is the head of an electric field vector starting at the origin (0,0). This shows that the electric field in the spin plane projects to the vertical direction.

[11] Figure 5 presents the same voltage data as seen in Figure 3, but here the scale has been expanded to show the fields below and above the layer. Below the NLC layer, from 85 to 86.5 s in Figure 5, we can see probe data during three spins of the rocket. These clean sine waves have the expected  $90^\circ$  phase shift due to the orthogonal orientation of the two axes. The Sun spike is clearly seen when any probe goes into the shadow of the rocket. When the probe is shadowed, photoemission from the probe surface stops, and the probe becomes more negatively charged than when it is

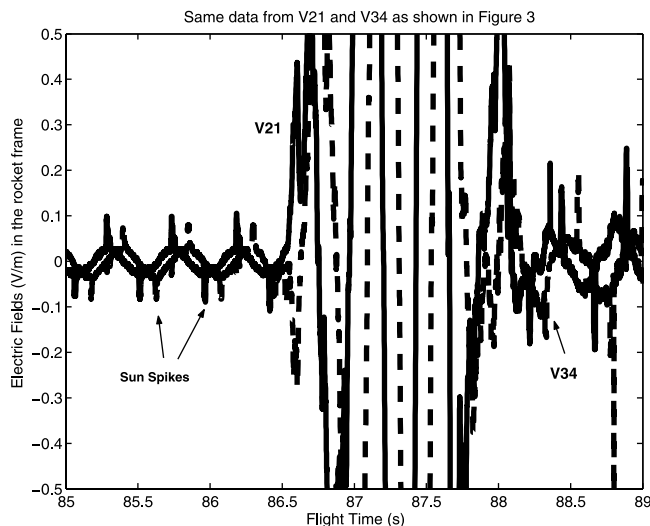


**Figure 5.** Same potential difference data as in Figure 3, but now the scale is expanded to see the clean  $\mathbf{v} \times \mathbf{B}$  electric field signal below and above the NLC.

in sunlight [see Mozer, 1973]. In Figure 5, this is seen as a negative spike for  $V_2$  or  $V_3$  in shadow and as a positive spike for  $V_1$  or  $V_4$  in shadow (because this plot is for the difference  $V_{2-1} = V_2 - V_1$  and  $V_{3-4} = V_3 - V_4$ ). The magnitude of the quasi-DC electric field we deduce from these sine wave data below the NLC layer is  $\sim 33 \text{ mV m}^{-1}$ . This is the electric field expected in the moving (rocket) frame  $\mathbf{E}' = \mathbf{E} + \mathbf{v} \times \mathbf{B}$  caused by the rocket motion across the magnetic field. In this case the  $\mathbf{v} \times \mathbf{B}$  field (caused by the  $\sim 1000 \text{ m s}^{-1}$  rocket velocity, which is nearly perpendicular to  $\mathbf{B}$ ) is  $\sim 30 \text{ mV m}^{-1}$  in the magnetic southwest direction, inclined substantially vertically downward, in full agreement with the low-amplitude sine wave data in Figure 5. Another feature to point out in Figure 5 is that just above the NLC layer the Sun spikes are nearly twice the magnitude as below the layer. This might be caused by the increased photoemission above the NLC if some UV sunlight was scattered or reflected by the NLC, reducing the amplitude in and below the NLC. This is the case for the wavelengths used by the photometers [see Gumbel, 2001], which are clearly reduced in magnitude in and below the NLC.

[12] Strong support for our interpretation of these data is obtained when we ask the question of whether fields determined by shorter booms give the same magnitude and direction. In Figure 6 we have added the voltage differences  $V_{2-6} = V_2 - V_6$  and  $V_{5-1} = V_5 - V_1$  to compare with the field determined by  $V_{2-1}$  (refer to Figure 2 for boom lengths). Since the total boom length of  $V_{5-1}$  plus that of  $V_{2-6}$  is just 1.2 m, we must compare fields and not voltages determined by these two techniques (so the different lengths are divided out). Also, we note that the voltages  $V_{5-1}$  and  $V_{2-6}$  have an electronic channel gain of 10.0, which

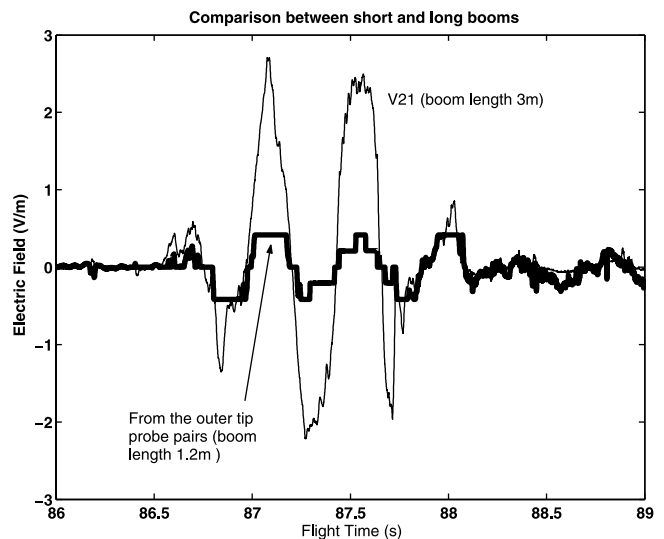


**Figure 6.**  $V_{2-1}$  (from Figure 3) compared to the sum of the voltage drops seen between the two pairs of voltage probes  $V_{2-6}$  and  $V_{5-1}$  (refer to Figure 2). These voltages have a baseline of just 1.2 m total, but when the different telemetry (TM) gains as well as the boom lengths are taken into consideration, both  $V_{2-1}$  and  $V_{2-6} + V_{5-1}$  give the same electric field up to the TM limit of the  $V_{5-1}$  and  $V_{2-6}$  measurements ( $\sim 500 \text{ mV m}^{-1}$ ).



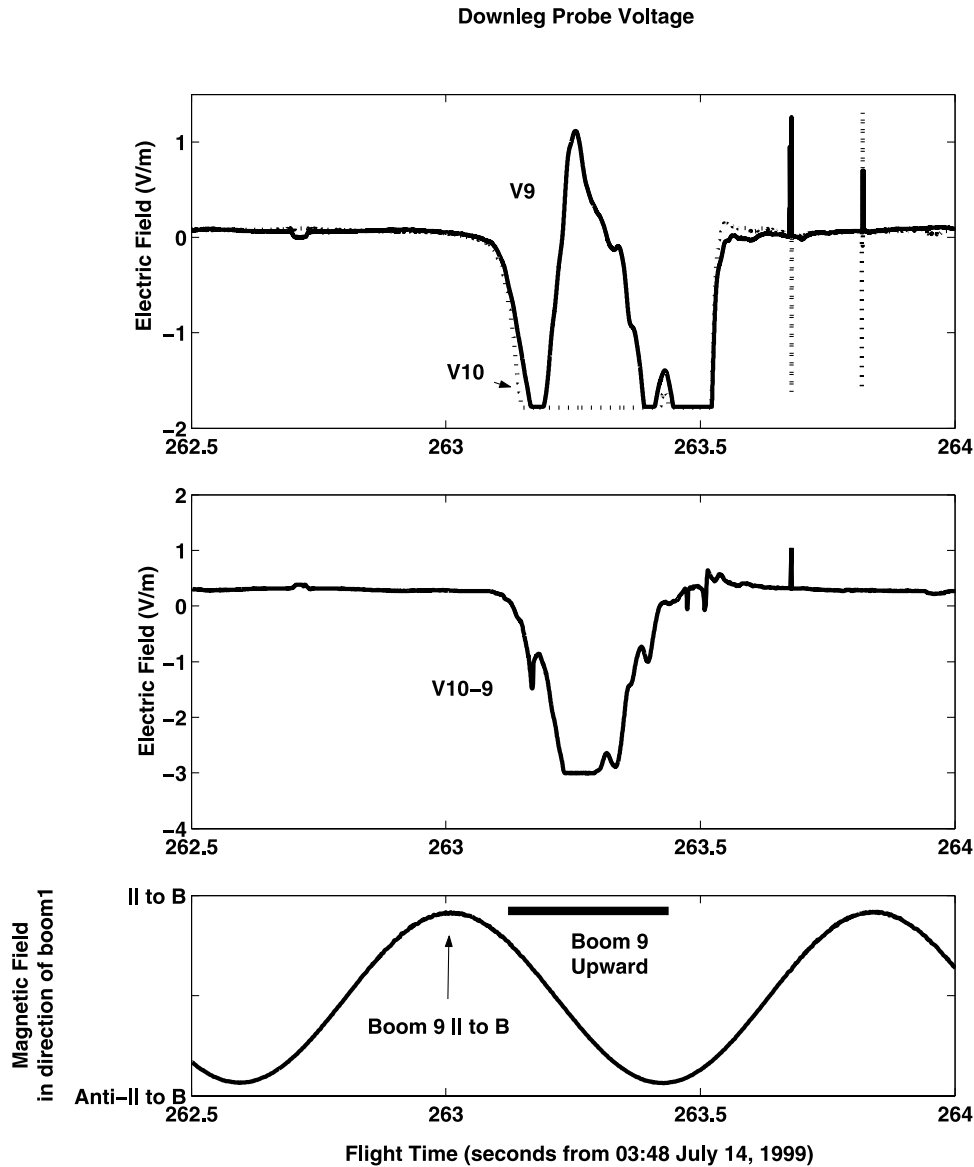


**Figure 7.** Downleg data of the aft probe voltages  $V_9$  and  $V_{10}$  as well as  $V_{10-9}$  along with the aspect magnetic field data during the NLC passage. Although the NLC encounter is brief, the probe voltages also show a vertical electric field of the same size as found on the upleg. These data also show that some probes went negative, as expected for the large fields and not consistent with a wake.

is 40 times that of  $V_{2-1}$ . So,  $V_{5-1}$  and  $V_{2-6}$  go out of telemetry (TM) range at much smaller electric fields than the fields which can be measured by  $V_{2-1}$ . In Figure 6 we see that the two signals track well up to  $\pm 0.5 \text{ V m}^{-1}$ , beyond which the signal from  $V_{2-6} + V_{5-1}$  is beyond TM limits. Thus, again, we argue that the fields determined using  $V_{2-1}$  are consistent with another, independent set of voltage measurements with shorter boom lengths. Note that none of the data presented in Figures 3–5 were obtained from saturated probes. Even in Figure 6, the forward preamps did not become saturated; only the telemetry gain for these measurements caused the transmitted voltages to be out of the telemetry voltage range because of the very high gain for  $V_{2-6}$  and  $V_{5-1}$ .

[13] At this point it is important to mention that the equivalent measurements along the  $V_{3-4}$  boom axis give exactly the same conclusion as we obtain from Figures 5

and 6. So, probes from both forward axes provide completely consistent evidence for the large electric fields seen inside the NLC.

[14] The downleg data offer us another look at the fields within the NLC. The vehicle was reoriented into a nearly horizontal attitude, with the forward end  $\sim 10^\circ$ – $20^\circ$  above the horizontal. During the downleg the ballistic trajectory carried the rocket nearly parallel to the magnetic field, so the  $\mathbf{V} \times \mathbf{B}$  component of the field was nearly zero. Additionally, the rocket was spun down to just 1.2 s period. As it turns out, the NLC encountered on the downleg was much thinner than seen on the upleg. Whereas the upleg width was  $\sim 2 \text{ km}$ , the downleg width was only  $\sim 0.5 \text{ km}$ . So, the passage occurred in less than one-half of a rocket spin.

[15] Figure 7 presents the probe voltages for  $V_9$  and for  $V_{10}$  along with the magnetic field in the direction of

boom 9 during the NLC downleg passage. These aft probes  $V_9$  and  $V_{10}$  were now slightly lower, or more in the RAM direction, than were the forward booms. The fields were somewhat stronger than on the upleg but otherwise look very similar. In this case we are showing the aft probe pairs because they show us unequivocally that the big fields are not a wake artifact. To interpret Figure 7, note first that as the event grows, both  $V_9$  and  $V_{10}$  start out negative, not positive (as was seen on DROPPS1 in the wake). This is because they are on the aft end of the rocket, and in the presence of a vertical field the probes will both be at a lower voltage than the average of the rocket skin, even though at the initial roll position they are very nearly in the horizontal plane at the start of the event. Figure 7 shows that during the passage, boom 9 moved principally upward, boom 10 downward, and  $V_{10-9}$  measured a nice vertical electric field of similar magnitude to the upleg. It is also worth mentioning that all the other probes measured fields that were completely consistent with the interpretation we have given here. The convincing feature of these downleg data is that several of the probes actually went negative with respect to the rocket skin, which is not a signature of a wake; that is, if one supposed that the fields we measured were somehow caused by the wake, then we would expect the measured field to flip polarity on the downleg since the charged wake will then be above the rocket. As we can clearly see from Figure 7, the measured electric field on the downleg was also vertically downward, just like on the upleg, thus adding further evidence that the electric field we report is geophysical and not caused by the wake.

### 3. Discussion and Conclusions

[16] We have provided electric field measurements during both an up and down encounter of a strong noctilucent cloud during the DROPPS2 rocket experiment. Since measurement of mesospheric electric fields by rockets has been a controversial endeavor, we have primarily concentrated on providing technical evidence that our measurements were not unduly influenced by a vehicle wake. After first providing the raw measurements, from which we reported up to  $3 \text{ V m}^{-1}$  downward vertical electric field inside the NLC, we provided three arguments to support our interpretation. First, we pointed out that the instrument was, in fact, working properly at altitudes below and above the layer, where we clearly measured clean sine waves from the expected  $\mathbf{v} \times \mathbf{B}$  and geophysical electric field. We showed that electric fields determined by probes with two different boom lengths gave us the same electric field, which is also an argument that no vehicle potential perturbation strongly affected the probes. Then, we gave data from the downleg, where, even though the NLC encounter was very brief, it was nevertheless prime evidence that the probes were operating properly and were not affected by wake potentials. We note that only data from booms in the RAM direction and not in the vehicle wake were used. This means that on neither the upleg or downleg did we accurately measure more than two dimensions of the electric field. Note, however, that the boom orientation during the downleg was within  $13^\circ$  of vertical during the spin. These downleg  $V_{10-9}$  data were

completely consistent with the conclusion we reached using upleg, spin plane data, namely, that the field was vertically downward at  $2.5\text{--}3 \text{ V m}^{-1}$ .

[17] Here we take a preliminary look at other information we can derive from the measurements. In Figure 8 we both differentiate and integrate the measured vertical electric field with altitude. Figure 8 (top) is the measured vertical component of the electric field in the spin plane. Figure 8 (middle) is the charge density one would get from the gradient in the vertical electric field, i.e.,  $\rho = \epsilon_0 \nabla \cdot \mathbf{E}$ , where the abrupt shutoff of the electric field at the top boundary results in a charge density over  $2 \text{ pC m}^{-3}$ . If this were all in the form of positive, singly charged ions or aerosols, the charge number density would be over  $10^7 \text{ particles m}^{-3}$ . The actual layer is just 10 m thick, which we resolve quite easily with our high-speed telemetry data. Note that this is a measure of the net charge density, so actual number densities may be even larger if both positive and negative charges exist there.

[18] Such a large charge density layer could be maintained by, for instance, a vertical current density of just a few picoamperes per meter passing through a boundary between an upper region with high conductivity into a region (the NLC) with greatly reduced conductivity (due, for instance, to the enhanced presence of aerosols, to which the electrons are attached). As noted by *Goldberg et al.* [2001], the night of the DROPPS2 flight was magnetically very quiet, with no evidence from magnetometers or from the Eiscat radar of any auroral charged particle precipitation. Therefore if we speculate that the only vertical current was that due to the global circuit return current [cf. *Volland*, 1984], with vertical current density  $J$  and amplitude  $\sim 1 \text{ pA m}^{-2}$ , and if we assume that  $J$  is continuous through the NLC (because the NLC is very thin, with great horizontal extent), then we would suggest that the conductivity  $\sigma$  inside the NLC was on the order of

$$\sigma = J/E \approx 1 \times 10^{-12} \text{ A m}^{-2} / 2.5 \text{ V m}^{-1} = 4 \times 10^{-13} \text{ S m}^{-1}.$$

This is at least two orders of magnitude below the lowest expected conductivity at 85 km altitude and perhaps six orders below the usual daytime conductivity at 85 km [*Hale*, 1984]. The DROPPS gerdien condensor was not producing usable data on this flight (C. L. Croskey, personal communication, 2004), so we have no direct comparison for this deduced conductivity. However, from conductivity data on other flights, *Croskey et al.* [2001] have reported that during strong electron byte outs similar to the one seen on this DROPPS flight [*Croskey et al.*, 2001] the positive ion conductivity remains fairly constant at much higher values (say, near  $10^{-9} \text{ S m}^{-1}$ ). So, to have a conductivity as low as  $10^{-13} \text{ S m}^{-1}$  requires that the positive ion conductivity also be removed, leaving the measured charge density perhaps residing just on the aerosols. Remember, the charge density we determine arises strictly from the strong divergence of the electric field, seen in all probes at the same time. Such a steep cutoff of a strong electric field cannot occur in a steady state plasma without such a charge layer. Our estimate of the conductivity, given the charge density, scales with the assumed current density.

[19] The lower panel of Figure 8 is simply the integral of the vertical electric field through the NLC layer. This shows

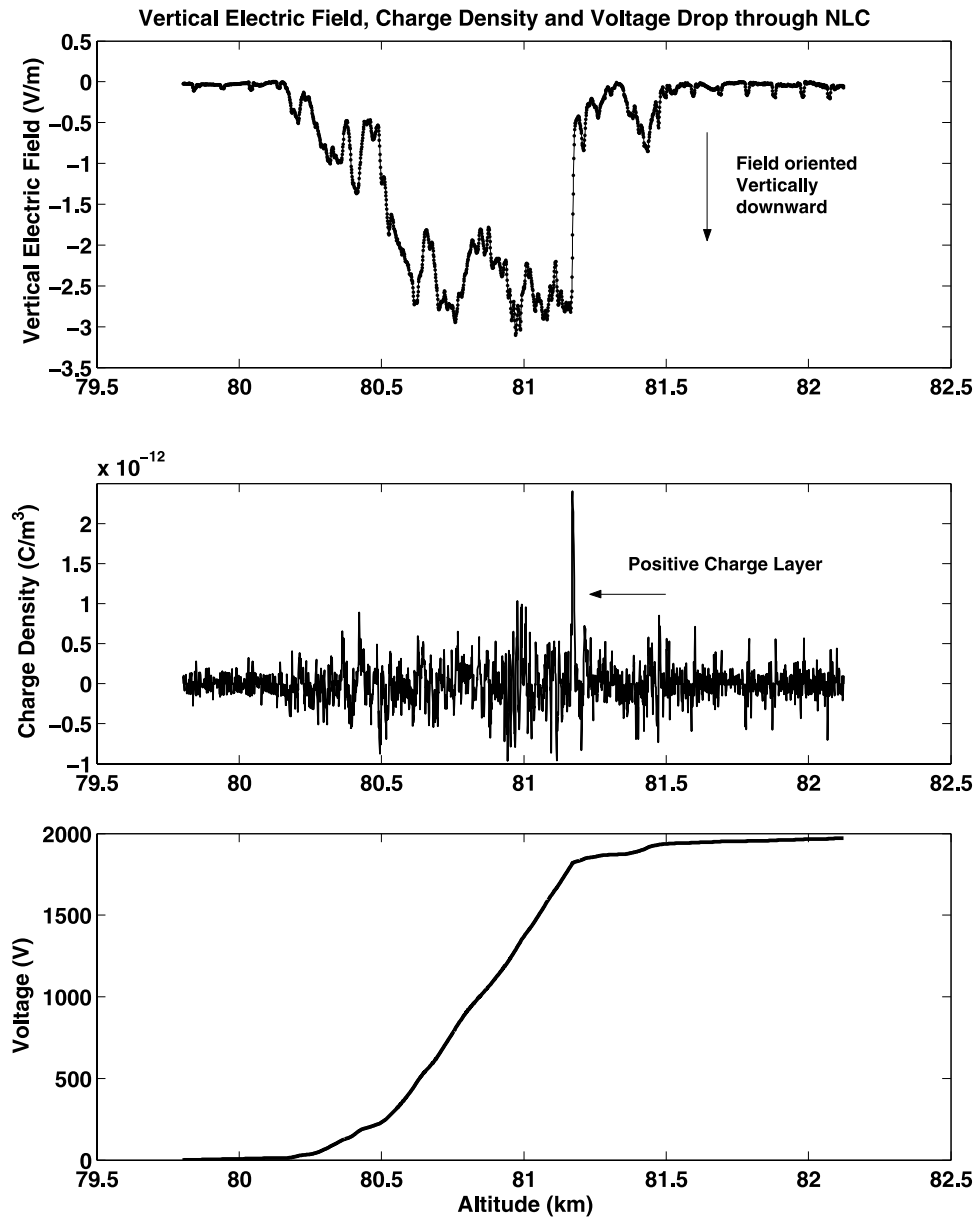


**Figure 8.** Charge density calculated from the field gradient and the total potential drop calculated from the field integral during the upleg encounter with the NLC. The peak charge density is over  $2 \text{ pC m}^{-3}$  and the total voltage drop is 2 kV.

that the total potential drop is  $\sim 2 \text{ kV}$  from top to bottom. This could be a powerful force to be included in ion and aerosol drift equations for NLC dynamics. This large field causes positively charged particles (ions and aerosols) to drift downward and the negatively charged aerosols (which gobbled up all the free electrons) to move up.

[20] From this analysis we conclude that the DROPPS2 rocket passed through an NLC in which existed a strong electric field oriented vertically downward. Detailed analysis of data from a variety of probes, including probes with differing baselines and during both upleg and downleg passes of the NLC, gave a consistent interpretation of the fields. The expected charged wake of the rocket as it passed through the NLC was not large enough to adversely influence our measurements. From the gradient in the electric field we estimate the peak, net, or excess charge

density at the top of the NLC to be  $2 \text{ pC m}^{-3}$ , confined to a narrow layer  $\sim 10 \text{ m}$  thick, and the total potential drop through the cloud to be 2 kV.

[21] **Acknowledgments.** The authors would like to thank Rob Pfaff, Jorg Gumbel, and Charlie Croskey for help with DROPPS2 aspect analysis and for important discussions. This work was supported in part by NASA grant NAG5-5183 and by the University of Washington with sabbatical support for R. Holzworth.

## References

- Cho, J. Y. N., and M. C. Kelley (1993), Polar mesosphere summer radar echoes: Observations and current theories, *Rev. Geophys.*, *31*(3), 243–265.
- Cho, J. Y. N., and J. Röttger (1997), An updated review of polar mesosphere summer echoes: Observation, theory, and their relationship to noctilucent clouds and subvisible aerosols, *J. Geophys. Res.*, *102*, 2001–2020.

- Croskey, C. L., J. D. Mitchell, M. Friedrich, K. M. Torkar, U.-P. Hoppe, and R. A. Goldberg (2001), Electrical structure of PMSE and NLC regions during the DROPPS program, *Geophys. Res. Lett.*, **28**, 1427–1430.
- Goldberg, R. A., et al. (2001), DROPPS: A study of the polar summer mesosphere with rocket, radar and lidar, *Geophys. Res. Lett.*, **28**, 1407–1410.
- Gumbel, J. (2001), Aerodynamic influences on atmospheric in situ measurements from sounding rockets, *J. Geophys. Res.*, **106**, 10,553–10,563.
- Hale, L. C. (1984), Middle atmosphere structure, dynamics and coupling, *Adv. Space Res.*, **4**(4), 175–186.
- Hale, L. C., C. L. Croskey, and J. D. Mitchell (1981), Measurements of middle-atmosphere electric fields and associated electrical conductivities, *Geophys. Res. Lett.*, **8**, 927–930.
- Holzworth, R. H., et al. (2001), Large electric potential perturbations in PMSE during DROPPS, *Geophys. Res. Lett.*, **28**, 1435–1438.
- Kelley, M. C., C. L. Siefring, and R. F. Pfaff Jr. (1983), Large amplitude middle atmospheric electric fields: Fact or fiction?, *Geophys. Res. Lett.*, **10**, 733–736.
- Maynard, N. C., C. L. Croskey, J. D. Mitchell, and L. C. Hale (1981), Measurement of volt/meter vertical electric fields in the middle atmosphere, *Geophys. Res. Lett.*, **8**, 923–926.
- Mitchell, J. D., C. L. Croskey, and R. A. Goldberg (2001), Evidence for charged aerosols and associated meter-scale structure in identified PMSE/NLC regions, *Geophys. Res. Lett.*, **28**, 1423–1426.
- Mozer, F. S. (1973), Analysis of techniques for measuring d.c. and a.c. electric field in the magnetosphere, *Space Sci. Rev.*, **14**, 272.
- Pfaff, R., et al. (2001), Rocket probe observations of electric field irregularities in the polar summer mesosphere, *Geophys. Res. Lett.*, **28**, 1431–1434.
- Rapp, M., and F.-J. Lübken (2003), On the nature of PMSE: Electron diffusion in the vicinity of charged particles revisited, *J. Geophys. Res.*, **108**(D8), 8437, doi:10.1029/2002JD002857.
- Rapp, M., F.-J. Lübken, P. Hoffmann, R. Latteck, G. Baumgarten, and T. A. Blix (2003), PMSE dependence on aerosol charge number density and aerosol size, *J. Geophys. Res.*, **108**(D8), 8441, doi:10.1029/2002JD002650.
- Volland, H. (1984), *Atmospheric Electrodynamics*, Springer-Verlag, New York.
- Zadorozhny, A. M., A. A. Tyutin, G. Witt, N. Wilhelm, U. Wälchli, J. Y. N. Cho, and W. E. Swartz (1993), Electric field measurements in the vicinity of noctilucent clouds and PMSE, *Geophys. Res. Lett.*, **20**, 2299–2302.

---

R. A. Goldberg, Laboratory for Extraterrestrial Physics, NASA Goddard Space Flight Center, Bldg 2, Room 225, Code 690, Greenbelt, MD 20771, USA. (goldberg@pop600.gsfc.nasa.gov)

R. H. Holzworth, Earth and Space Sciences, 310 Condon Hall, Box 351310, University of Washington, Seattle, WA 98195-1310, USA. (bobholz@u.washington.edu)